

Mesenchymal Stem Cell–Originated Exosomal Circular RNA circFBXW7 Attenuates Cell Proliferation, Migration and Inflammation of Fibroblast-Like Synoviocytes by Targeting miR-216a-3p/HDAC4 in Rheumatoid Arthritis

Lihua Chang¹
Liang Kan²

¹Department of Rheumatology and Immunology, Shengjing Hospital of China Medical University, Shenyang, Liaoning Province, People's Republic of China;

²Department of Gerontology and Geriatrics, Shengjing Hospital of China Medical University, Shenyang, Liaoning Province, People's Republic of China

Background: Rheumatoid arthritis (RA) is a chronic autoimmune disease of articular joint damage and elevated synovial hyperplasia. Abnormal proliferation, invasion inflammatory response of rheumatoid fibroblast-like synoviocytes (RA-FLS) play a critical role in RA progression. Mesenchymal stem cell (MSC)–derived exosomal circular RNAs are promising therapeutic manner for disease treatment. This work aimed to decipher the role of exosomal circFBXW7 in RA.

Methods: The expression of circFBXW7, miR-216a-3p, and HDAC4 were detected in clinical RA samples. The RA rat model was established. Isolation and identification of exosomes from MSCs was conducted. The effects of exosomal circFBXW7 on RA was evaluated by qPCR, CCK-8, transwell assays, flow cytometry, Western blotting, ELISA, and immunohistochemical assay. Interaction between miR-216a-3p and circFBXW7 or HDAC4 was determined by luciferase reporter gene assay and RNA pulldown.

Results: Exosomal circFBXW7 treatment suppressed proliferation, migration and inflammatory response of RA-FLSs and damage of RA model. CircFBXW7 could directly sponge miR-216a-3p to upregulate the expression of HDAC4. Inhibition of HDAC4 or upregulation of miR-216a-3p abolished the therapeutic function of exosomal circFBXW7. Our data demonstrated that circFBXW7 and HDAC4 were decreased, and miR-216a-3p was elevated in clinical RA sample compared with healthy samples.

Conclusion: We concluded that MSC-derived exosomal circFBXW7 suppressed proliferation, migration and inflammatory response of RA-FLSs and damage of RA rats via sponging miR-216a-3p and release the activation of HDAC4. These findings may provide a novel therapeutic target for RA.

Keywords: rheumatoid arthritis, mesenchymal stem cell, fibroblast-like synoviocytes, circFBXW7, miR-216a-3p, HDAC4

Introduction

Rheumatoid arthritis (RA) is a chronic autoimmune disease that severely affects the life quality of patients.¹ It is estimated that approximately 1% of the people around the world suffers from RA.¹ Noteworthy, as a typical inflammatory-related syndrome, RA progression is closely correlated with inflammatory responses,

Correspondence: Liang Kan
Department of Gerontology and Geriatrics, Shengjing Hospital of China Medical University, Shenyang, Liaoning Province, People's Republic of China
Email kanliang31cmu@163.com

especially the abnormal secretion of chemokines and cytokines.² RA is characterized by damage on articular joints caused by elevated synovial hyperplasia.¹ Therefore, RA development is closely associated with synovium function.³ Fibroblast-like synoviocytes (FLS) is the major component of synovium, and contributes to the homeostasis of joints via production of hyaluronan, lubricin, and plasminogen activator, as well as modulating the normal inflammatory responses in synovium.⁴ Nevertheless, rheumatoid FLSs (RA-FLSs) represent a unique aggressive form of FLSs, which exhibits boosted proliferation, invasion, and accumulation in articular joints.⁴

Mesenchymal stem cells (MSCs) are multipotent cells that have been suggested as potential therapeutic tools in clinical application such as modulating tissues repairment, inflammation, as well as immune response.^{5–9} Increasing evidences have implied the positive function of MSCs for RA treatment.^{10,11} Recent studies demonstrated that MSCs function through secreting soluble factors, and extracellular vehicles such as exosomes.¹² Exosomes are small (30–150 nm) membranous spherical vesicles with size around 30–150 nm, which deliver signaling factors between cells, and are involved in multiple cellular behaviors such as cell growth, differentiation, and apoptosis and so on.^{13–15} Circular RNAs (circRNAs) are novel form of noncoding RNAs with covalently closed sequence, and usually act as competing endogenous RNA of microRNAs (miRNAs) to regulate gene expression.¹⁶ Studies have exposed the therapeutic function of circRNAs that delivered by exosomes in diseases.^{17,18} CircFBXW7 are recently reported to suppress cell progression of breast cancer, glioma, and lung cancers, via sponging miRNAs.^{19–21} Importantly, circFBXW7 can be transferred by exosomes to regulate cancer progression.²² Meanwhile it has been identified that miRNAs, such as miRNA-486-5p, miRNA-4701-5p, and miRNA-146a, were involved in the regulation of RA progression.^{23–25} However, the function of miR-216a-3p in RA is still elusive.

Histone deacetylase 4 (HDAC4) belongs to class IIa histone deacetylase and functions as an epigenetic modifier enzyme.²⁶ Studies have been implicated the regulatory role of HDAC4 in multiple diseases such as cancers, neurodegenerative diseases, and ischemic stroke and so on.^{27–29} Noteworthy, a recent study suggested that HDAC4 suppressed progression of RA by hindering inflammatory cytokine production of RA-FLSs,³⁰ suggesting the vital function of HDAC4 in RA development.

In this study, we deciphered the role of exosomal circFBXW7 in RA progression and demonstrated that circFBXW7 suppressed proliferation, migration and invasion, as well as inflammatory response of fibroblast-like synoviocytes, possibly through sponging miR-216a-3p and elevating HDAC4 expression. Our findings provided circFBXW7/miR-216a-3p/ HDAC4 regulatory axis as novel therapeutic target for RA.

Materials and Methods

Collection of Clinical Synovial Tissues

To determine the expression of circFBXW7, miR-216a-3p, and HDAC4 in RA patients, we collected synovial tissues from 30 patients with RA and 30 healthy donors. The synovial tissues of RA groups were collected from RA patients who underwent synovectomy of the knee joint or knee replacement surgery. The synovial tissues of healthy control groups were taken from four patients who underwent arthroscopic surgery for knee meniscus injuries or cruciate ligament rupture and who had no medical history of acute or chronic joint abnormalities or systemic disease. All participants have signed the informed consents. Experiments in this study were authorized by the Ethics Committee of Shengjing Hospital of China Medical University, and were conducted in accordance with the Declaration of Helsinki. The diagnosis of RA followed the ACR/EULAR criteria.

Cell Lines

Human synovial cell line MH7A and human bone marrow-derived MSCs were obtained from Beijing Institute for Cancer Research Collection (China). MH7A cells were maintained in DMEM (Hyclone, USA) medium that supplemented with 10% FBS (Hyclone) and 1% penicillin/streptomycin at 37°C with 5% CO₂. MSCs were cultured in MEM (Hyclone) that supplemented with 10% FBS and 1% penicillin/streptomycin.

Cell Transfection

The circFBXW7 and HDAC4 overexpressing vectors, short hairpin RNA (shRNA) targeting circFBXW7 and HDAC4, miR-216a-3p mimics and inhibitor, and negative control shRNA (shNC) were obtained from Shanghai GenePharma (China). Cell transfection was performed by using Lipofectamine 2000 (Invitrogen, USA) in accordance with manufacturer's instruction and miR-216a-3p.

Isolation and Identification of Exosomes

Exosomes were extracted from the culture medium of MSCs using a sequentially centrifuge method.³¹ The obtained exosomes were suspended in PBS and stored at -80°C for the subsequent experiments. Exosomes were used at concentration of $100\ \mu\text{g}/\text{mL}$ for in vitro experiments. Concentration of exosomes were detected by BCA kit (Beyotime, China). The nanoparticle tracking analysis (NTA) was performed to measure particle size on a Nanosight NS300 analyzer (Malvern Instruments Ltd, UK).

Fluorescence in situ Hybridization Assays

To determine the intracellular localization of circFBXW7, we conducted FISH assay. In brief, MSCs were fixed and dehydrated, stained with Cy3-labeled probes that target U6, 18s, or circFBXW7 (GenePharma, USA). The U6 probe was taken as representative of nuclear localization, and 18s probe as reference of cytoplasmic localization. The fluorescence was observed under a confocal fluorescence microscope (Leica, Germany).

Internalization of Exosomes

The exosomes obtained from MSCs were labeled by fluorescent dye Dil (Invitrogen) following the manufacturer's protocol, and administrated to MH7A cells to incubate for 6 and 24 hours. The nucleus was dyed with DAPI. Positive staining was captured by a confocal fluorescence microscope (Leica).

Establishment of RA Model in Rats

Lewis rats aged 6-week-old (180–210g) were brought from Vital River Laboratory Animal Technology Co., Ltd. (China), and were randomly grouped. Rats in RA model group were intradermally injected with Freund's adjuvant which consists of heat-killed clostridium butylicum and mycobacterium suspended in mineral oil at a dose of $25\ \text{mg}/\text{kg}$. The pure mineral oil was injected into rats in the control group. For the treatment group, rats were injected with exosomes ($100\ \mu\text{g}$) or oligonucleotides ($200\ \mu\text{g}$). The RA degree was scored as following standard:

0–1 point: no detectable pathology normal appearance with a flexible and evasive body;

1–2 points: arthritis onset slight swelling of the joint;

2–4 points: mild arthritis swollen joint with inflammation;

4–6 points: mild-to-moderate arthritis swollen joint; last finger deformed inward; the paw could transiently support the body weight; decreased flexibility and grip strength;

6–8 points: severe arthritis severe swelling of joint, paw, and finger; deformation of joints and legs; lack of support in the upper part; loss of weight; lack of flexibility and no grip strength; climbing and feeding affected;

All research of animals was rigorously carried out according to the National Institutes of Health guide for the Care and Use of Laboratory Animals and international ethical guidelines. All animal experiments were approved by the Ethics Committee of Shengjing Hospital of China Medical University.

Real-Time PCR

Cells, exosomes, and synovial tissues were lysed to extract total RNA by using the TriZol reagent (Thermo). The cDNA was synthesized by First Strand cDNA synthesis mixture (Transgen, China). The relative levels of circFBXW7, miR-216a-3p, and HDAC4 were detected by using SYBR Premix TaqTM II Kit (Thermo) in line with the manufacturer's instruction, using the $2^{-\Delta\Delta\text{Ct}}$ method. GAPDH and U6 were adopted as the internal control.

Cell Proliferation and Apoptosis

The viability and proliferation of MH7A cells was detected by Cell Counting Kit 8 (CCK-8, Thermo) assay and EdU staining following the manufacturer's instruction. For CCK-8, cells were seeded in 96-well plates at a density of 5000 cells per well after indicated transfection. At specific time points, $10\ \mu\text{L}$ CCK-8 solution was added and the absorbance values were recorded by a microplate detector (BD Biosciences, USA). For EdU detection, the fresh medium that contains EdU reagent was added to hatch with cells in 96-well plates for 10 hours, then fixed by 4% polyformaldehyde (PFA). The nucleus was stained with DAPI. The images were captured by a fluorescence microscopy (Leica, Germany). To detect cell apoptosis, MH7A cells were collected after indicated treatment, suspended in binding buffer, followed by staining with FITC-Annexin V and PI solution (Thermo, China) for 30 minutes in dark. The samples were analyzed by using a FACS flow cytometer (BD Biosciences, USA).

Cell Invasion and Migration

The invasion and migration of MH7A cells was detected by using transwell and wound healing assays. For

transwell assay, cells were suspended in FBS-free medium and seeded in Matrigel-covered upper chambers, the lower chambers were added with complete culture medium with 10% FBS. After incubation for 24 hours, the cells invaded from upper chambers were stained with 0.2% crystal violet for 20 minutes, and photographed by a microscope. For wound healing assay, cells were seeded in 6-well plates to form monolayer, then scratch by a 200- μ L pipette tip and washed with PBS to remove debris. The width of wound was captured at 0 and 48 hours by a microscope (Leica).

Western Blotting Assay

Cells, exosomes, and synovial tissues were lysed with RIPA lysis buffer (Thermo, USA) to extract total proteins. An equal amount of 35 μ g proteins were loaded and divided by SDS-PAGE, blotted to PVDF membranes. The blots were blocked in 5% non-fat milk, followed by incubation with primary antibodies against CD63, CD81, TSG101, GPR94, HDAC4, p-I κ B α , p52, RELB, and GAPDH overnight at 4°C. Next day, the proteins were incubated with HRP-conjugated secondary anti-mouse or anti-rabbit antibodies, and visualized by using ECL reagent (Sigma) in a gel image system (BD Bioscience). All antibodies were purchased from Abcam (USA) and used following manufacturer's description.

Enzyme Linked Immunosorbent Assay

The secreted levels of cytokines including the CCL2, CXCL5, CXCL1, TNF- α , IL-6, IL-1 β , IL-8, and CXCL8 were measured by performing Meso Scale Discovery (MSD) assay in line with the manufacturer's description on a QuickPlex SQ120 system (MSD, USA).

Immunohistochemical Analysis

The synovial tissues were isolated from rats, fixed, dehydrated, embedded into paraffin, and sliced into 5 μ m thickness sections. The samples were subjected dewaxing, antigen retrieval, and incubation with primary anti- β -catenin (1:200, Abcam) and anti-c-Myc (1:200, Abcam) antibodies. Next day, the target proteins were visualized after incubation with biotin-labeled secondary antibodies (Abcam). Five random areas were captured by microscope.

RNA Pulldown

Biotin-labeled miR-216a-3p probe was purchased from GenePharma (China) and conjugated with Dynabeads (Invitrogen, USA). MH7A cells were lysed, sonicated,

and hatched with the probes overnight at 4°C. Enrichment of circFBXW7 was determined by qRT-PCR assay.

Luciferase Reporter Gene Assay

The wild-type (WT) or mutant (MUT) sequences of circFBXW7 or HDAC4 3'UTR were synthesized and cloned into pmirGLO vectors. MH7A cells were seeded in 12-well plates, co-transfected with miR-216a-3p mimics or negative control, and the WT or MUT plasmids for 48 hours. Subsequently, the Dual-Luciferase Reporter Assay System (Promega, USA) was used to determine the luciferase activity.

Statistics

Data were presented as mean \pm SD and analyzed using the SPSS software (Version 20.0). Statistical significance was analyzed by Student's *t* test or one-way ANOVA for comparison among two or more groups. $P \leq 0.05$ was set as statistically significant.

Results

CircFBXW7 Could Be Delivered from MSCs to Fibroblast-Like Synoviocytes by Exosomes

To determine the role of MSCs-derived exosomes during RA, we first isolated MSCs from rats and extracted exosomes from the culture medium. The positive staining of CD44, CD105, and CD73 and negative expression of CD31, CD34, and CD45 (Figure 1A) on cell surface verified the features of MSCs. Exosomes were then obtained from the culture medium of MSCs (Figure 1B). The characterization of exosomes was exhibited by abundance of CD63, CD81, and TSG101 biomarkers and lack of GPR94 (Figure 1C), as well as the particle size that distributed around 100 nm (Figure 1D). Besides, the presence of Dil-labeled exosomes in cytoplasm indicated the time-dependent internalization of MSC-derived exosomes by MH7A cells (Figure 1E). We next conducted the characterization of circFBXW7. We observed that circFBXW7 was detectable under the treatment of RNase R, and the linear FBXW7 RNA was not detectable (Figure 2A). Besides, the half-life of circFBXW7 under actinomycin D treatment was notably higher than that of linear FBXW7 (Figure 2B). Further FISH assays revealed that Cy3-labeled circFBXW7 localized in cytoplasm of MSCs (Figure 2C). To further confirm that circFBXW7 could be

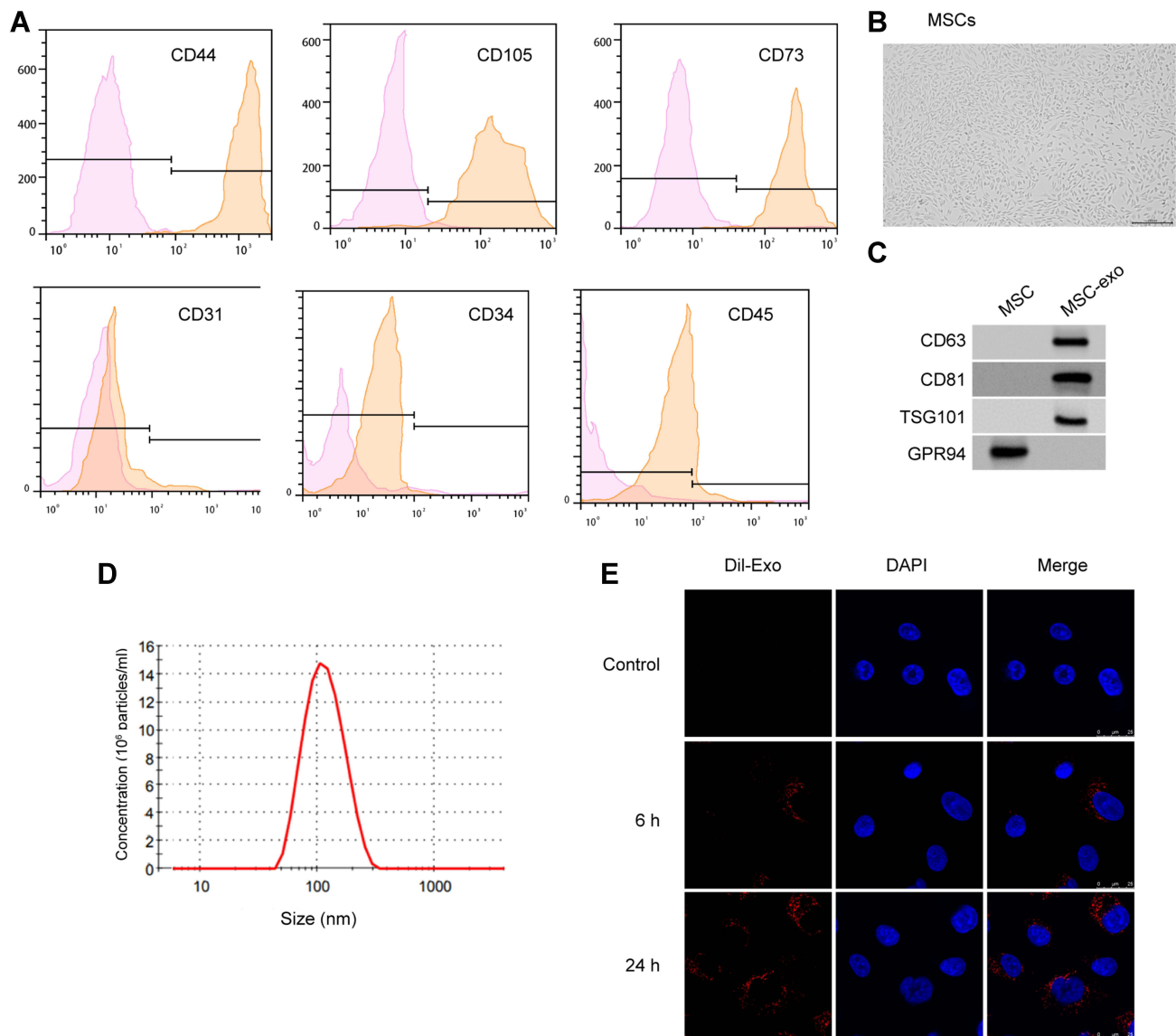


Figure 1 Identification of MSC-derived exosomes. **(A)** Flow cytometry to check the expression of cell surface markers CD44, CD105, CD73, CD31, CD34, and CD45 on MSCs. **(B)** The morphology of MSCs examined by microscope. **(C–E)** Western blotting to detect protein biomarkers of exosomes. Nanoparticle tracking analysis (NTA) to measure the size distribution of exosomes. X-axis, size of exosomes (nm). Y-axis, particle concentration in 1 mL PBS. Internalization of Dil-labeled exosomes (red) by MH7A cells. Blue, DAPI staining of nucleus.

delivered from MSCs to MH7A cells by exosomes, we conducted ectopic expression and depletion of circFBXW7 in MSCs. We demonstrated that overexpression of circFBXW7 caused increased level of circFBXW7 in MSCs and the MSCs-derived exosomes (Figure 2D). Incubation with exosomal-circFBXW7 also elevated the level of circFBXW7 in MH7A (Figure 2E). Consistently, knockdown of circFBXW7 with shcircFBXW7-1 and shcircFBXW7-2 in MSCs led to notably decreased level of circFBXW7 in MSCs, MSCs-derived exosomes and the incubated MH7A cells (Figure 2F and G). The shcircFBXW7-1 was applied for the following study.

Meanwhile, the circFBXW7 expression was repressed in the exosomes from the serum of RA patients compared with control samples (Figure 2H).

Exosomal-circFBXW7 Suppresses Proliferation and Migration of Fibroblast-Like Synoviocytes

We next determined the role of exosomal circFBXW7 on the functions of fibroblast-like synoviocytes in vitro. The effective internalization of exosomal circFBXW7 by MH7A cells was determined by qRT-PCR (Figure 3A). Treatment with exosomal-circFBXW7 notably suppressed the viability

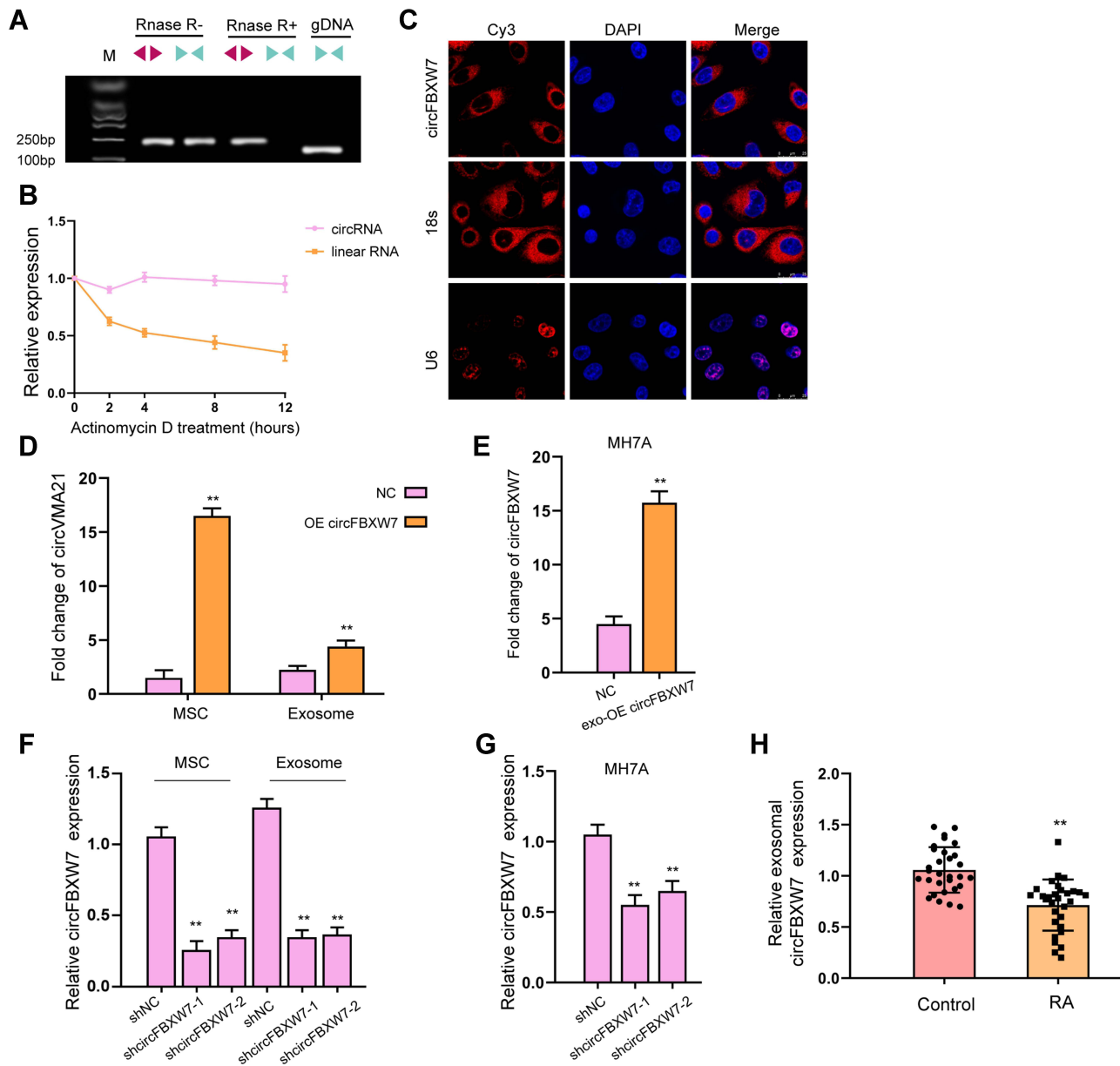


Figure 2 Identification and internalization of circFBXW7. **(A)** The levels of back-spliced and canonical forms of FBXW7 MSCs with or without RNase R treatment were detected by PCR and agarose gel electrophoresis assay. **(B)** The half-life of linear or circular form of FBXW7 RNA under actinomycin D treatment. **(C)** The localization of circFBXW7 was determined by FISH analysis and 18s and U6 were the controls. **(D)** MSCs were transfected with circFBXW7 overexpressing vectors, the level of circFBXW7 in MSCs and MSC-derived exosomes was detected by qRT-PCR. **(E)** The circFBXW7 level in MH7A cells after incubation with exosomes isolated from MSCs that transfected with circFBXW7 overexpressing vectors (exo-circFBXW7) or empty vectors (NC). **(F)** MSCs were transfected with shcircFBXW7, the level of circFBXW7 in MSCs and MSC-derived exosomes was detected by qRT-PCR. **(G)** The circFBXW7 level in MH7A cells after incubation with exosomes isolated from MSCs that transfected with shcircFBXW7 or negative control (NC). **(H)** The expression of circFBXW7 was measured qPCR in the exosomes from the serum of RA patients. ** $P < 0.01$.

(Figure 3B), proliferation (Figure 3C), invasion and migration (Figure 3D and E), as well as enhanced cell apoptosis (Figure 3F). In addition, the levels of TNF- α , IL-1 β , IL-6 and IL-8 was suppressed by the administration of exosomal-circFBXW7 (Figure 3G). However, we failed to observe the effect of exosomal-FBXW7 on the proliferation and migration of fibroblast-like synoviocytes in vitro (Figure S1).

Exosomal-circFBXW7 Alleviates RA and Inflammation in vivo

To further confirm the effect of exosomal circFBXW7 on RA in vivo, we constructed a RA rat model and treated the rats with exosomal circFBXW7. The administration of exosomal circFBXW7 ameliorated the pathological injury of the RA rats (Figure 4A). The immunohistochemical

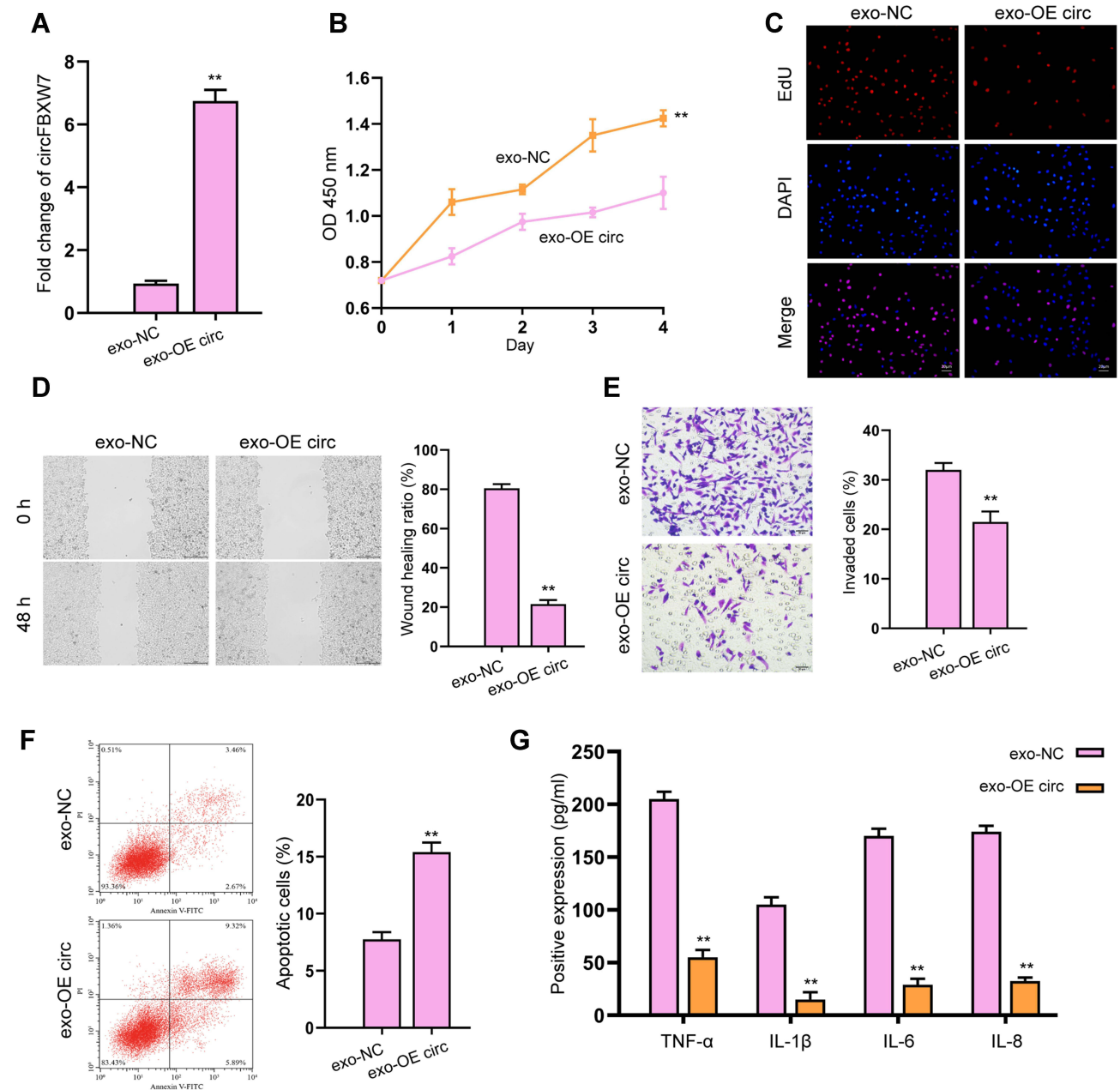


Figure 3 Exosomal-circFBXW7 suppresses proliferation and migration of fibroblast-like synoviocytes. The MH7A cells were treated with exosomes isolated from circFBXW7 transfected MSCs (exo-OE circ). **(A and B)** The expression of circFBXW7 was analyzed by qPCR. The cell viability was checked by CCK-8 assays. **(C)** The cell proliferation was measured by EdU assays. **(D and E)** The cell invasion and migration were determined by transwell and wound healing assay **(E)**. **(F)** Cell apoptosis was measured by flow cytometry. **(G)** The levels of TNF- α , IL-1 β , IL-6 and IL-8 were analyzed by ELISA assay. ** $P < 0.01$.

staining indicated that β -catenin and c-Myc expression were suppressed by exosomal circFBXW7 (Figure 4B). Moreover, the exosomal circFBXW7 notably inhibited the secretion of inflammation factors, including TNF- α , IL-1 β , IL-6, and IL-8 (Figure 4C).

CircFBXW7 Acts as ceRNA of miR-216a-3p to Modulates Fibroblast-Like Synoviocytes Proliferation and Migration
Subsequently, we determined the possible downstream factors of circFBXW7 in fibroblast-like synoviocytes. We

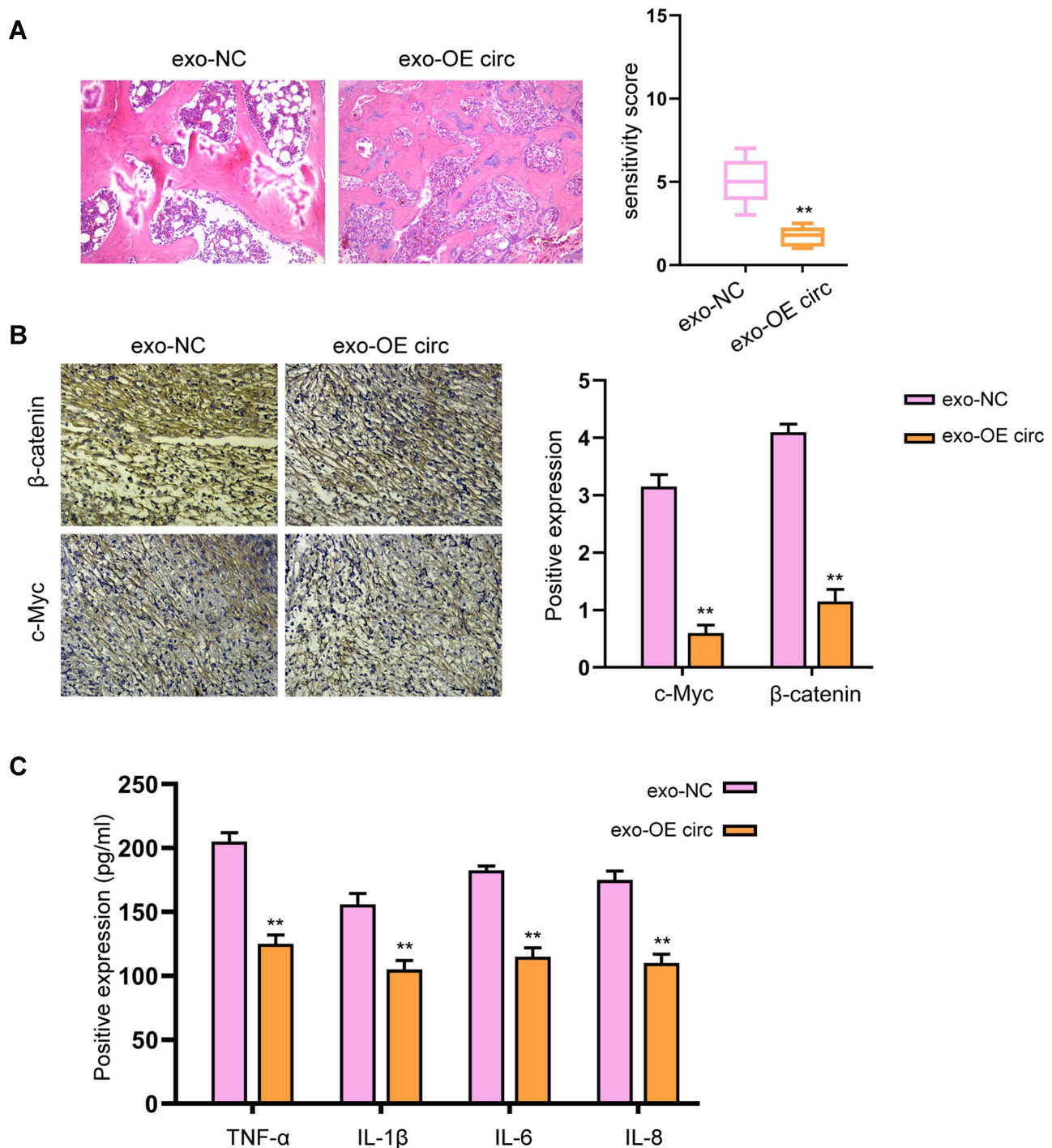


Figure 4 Exosomal-circFBXW7 alleviates RA and inflammation in vivo. The RA rat model was constructed and treated with exosomal circFBXW7 (exo-OE circ) or negative control (exo-NC). **(A)** The pathological changes were analyzed by H&E staining. **(B)** The levels of β -catenin and c-Myc in synovium were measured by immunohistochemical staining. **(C)** The levels of TNF- α , IL-1 β , IL-6, and IL-8 were checked by ELISA assay. ** $P < 0.01$.

found that miR-216a-3p could interact with the wild-type circFBXW7 rather than the mutated sequences, manifested by decreased luciferase activity of reporter gene vectors (Figure 5A and B). Notably, RNA pulldown analysis identified the direct interaction of circFBXW7 with miR-

216a-3p, suggested by the enrichment of circFBXW7 by biotin-labeled miR-216a-3p rather than the miR-216a-3p mutant (Figure 5C). The knockdown of circFBXW7 upregulated the expression of miR-216a-3p in MH7A cells (Figure 5D). Moreover, administration of miR-216a-3p

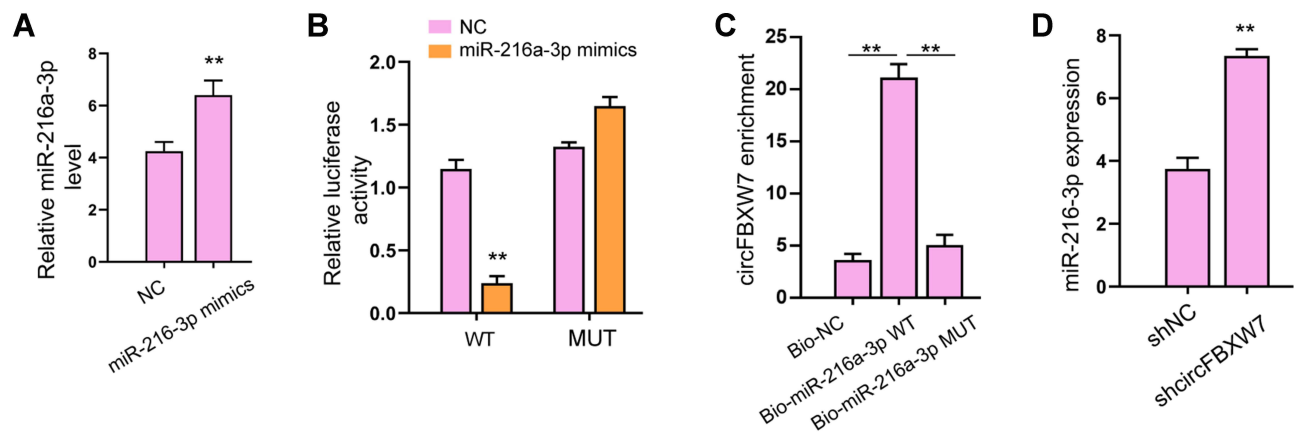


Figure 5 CircFBXW7 acts as sponge of miR-216a-3p. (A and B) The HCT-116 and HT-29 cells were treated with miR-520a-5p mimic. The expression of miR-520a-5p was validated by qPCR.²³ The luciferase activity of circFOXPI and circFOXPI mutant was analyzed by dual-luciferase reporter assay. (C) The interaction of miR-520a-5p and circFOXPI was analyzed by RNA pull down. (D)²⁵ The expression of miR-520a-5p was determined by qPCR in HCT-116 and HT-29 cells treated with circFOXPI shRNA. ** $P < 0.01$.

reversed the suppressed cell viability, proliferation, migration and invasion (Figure 6A–C), and ameliorated the stimulated apoptosis (Figure 6D) of MH7A cells. The secretion of inflammatory factors was also recovered by miR-216a-3p treatment (Figure 6E).

miR-216a-3p Targets HDAC4 3'UTR to Modulate Fibroblast-Like Synoviocytes Behaviors and Inflammatory Response in RA

We next determined the interaction between miR-216a-3p and HDAC4 3'UTR. As shown in Figure 7A, the luciferase activity of wild-type HDAC4 3'UTR, but not the mutated-type, was downregulated by miR-216a-3p. MiR-216a-3p treatment notably suppressed HDAC4 expression in MH7A cells (Figure 7B). Consistently, knockdown of circFBXW7 suppressed the expression of HDAC4, whereas inhibition of miR-216a-3p reversed this effect (Figure 7C). Noteworthy, the level of phosphorylated I κ B- α was upregulated by miR-216a-3p inhibitors, whereas the p52 and RELB levels were reduced (Figure 7D and E). Besides, the expression of CXCL5, CXCL8, CXCL1, and CCL2 were stimulated by miR-216a-3p, whereas the overexpression of HDAC4 abolished this phenomenon (Figure 7F). CCK-8 assays indicated that the administration of miR-216a-3p stimulated cell proliferation, and the overexpression of HDAC4 abolished this effect (Figure 8A). Moreover, miR-216a-3p inhibition suppressed the proliferation and invasion of MH7A cells,

stimulated cell apoptosis, as well as suppressed secretion of inflammatory factors, whereas knockdown of HDAC4 rescued the phenotype (Figure 8B–E).

circFBXW7 Modulates RA Progression via miR-216a-3p/HDAC4 Axis

Next, we evaluated the *in vivo* function of circFBXW7/miR-216a-3p/HDAC4 axis in RA rats. As shown in Figure 9A and B, knockdown of HDAC4 abolished the therapeutic effect of exosomal circFBXW7 in the pathological injury of the RA rats. The immunohistochemical analysis indicated that β -catenin and c-Myc expression were elevated by siHDAC4 under treatment with exosomal circFBXW7 (Figure 9C). The elevated level of phosphorylated I κ B- α , and suppressed p52 and RELB caused by exosomal circFBXW7 were reversed by HDAC4 inhibition (Figure 9D and E). Moreover, the depletion of HDAC4 notably stimulated the secretion of inflammation factors, including TNF- α , IL-1 β , IL-6, and IL-8, and abolished the effect of exosomal circFBXW7 (Figure 9F). Noteworthy, we analyzed the levels of circFBXW7, miR-216a-3p and HDAC4 in patients with RA. Consistent with our findings, the levels of circFBXW7 and HDAC4 were decreased in patients with RA, whereas the level of miR-216a-3p was elevated (Figure 9G). The correlation analysis indicated that level of miR-216a-3p was negatively correlated with circFBXW7 and HDAC4 expression, and circFBXW7 and HDAC4 were positively correlated (Figure 9H).

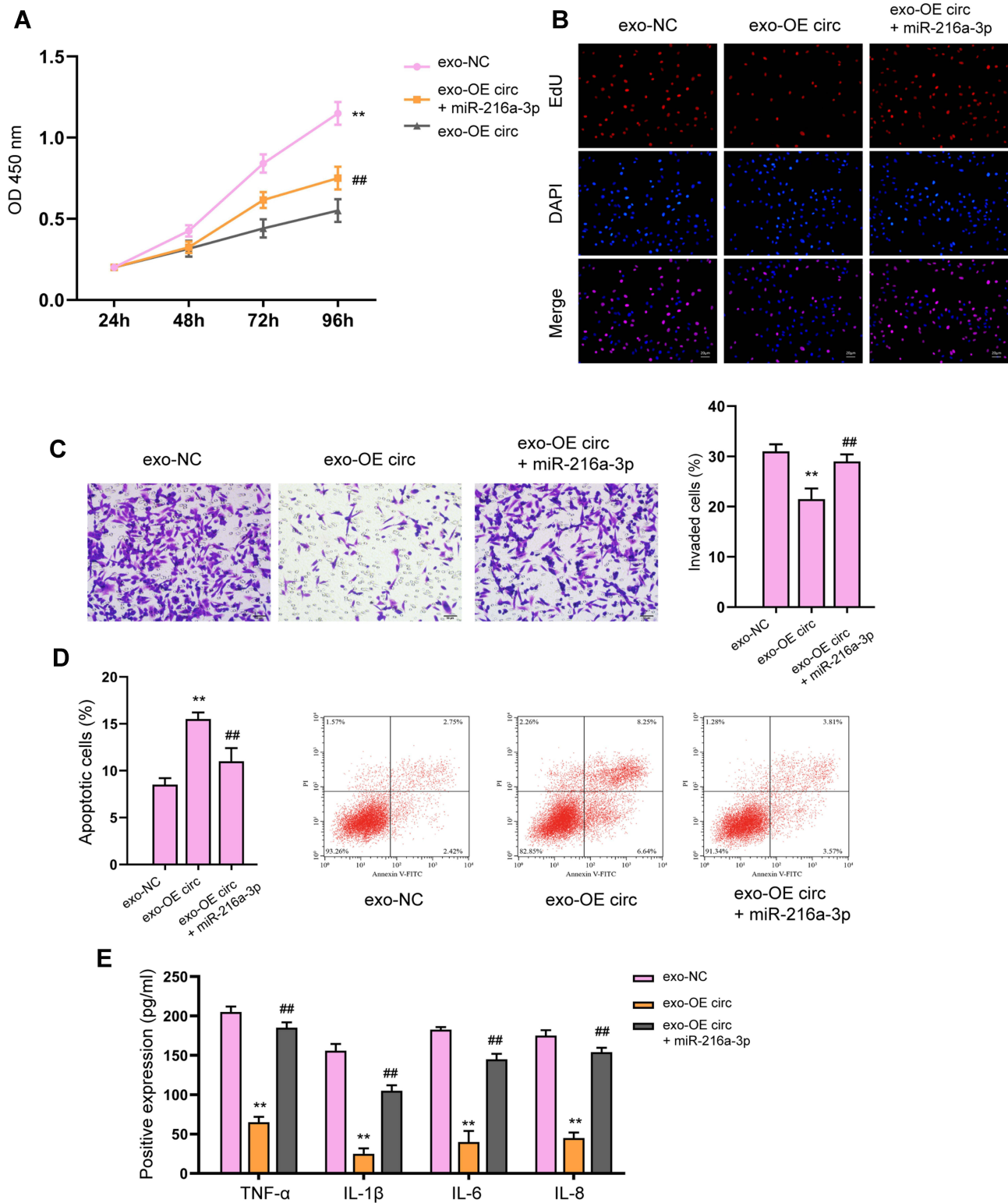


Figure 6 miR-216a-3p reverses circFBXW7-regulated fibroblast-like synoviocytes proliferation and migration. The MH7A cells were treated with exosomes isolated from circFBXW7 transfected MSCs along with miR-216a-3p mimics or negative control (NC). **(A)** Cell viability was measured by CCK-8 assay. **(B)** Cell proliferation detected by EdU assay. **(C)** The cell invasion was assessed by transwell. **(D)** Cell apoptosis determined by flow cytometry. **(E)** The levels of TNF- α , IL-1 β , IL-6 and IL-8 were analyzed by ELISA assay. ** $P < 0.01$ vs exo-NC, ## $P < 0.01$ vs exo-OE circ.

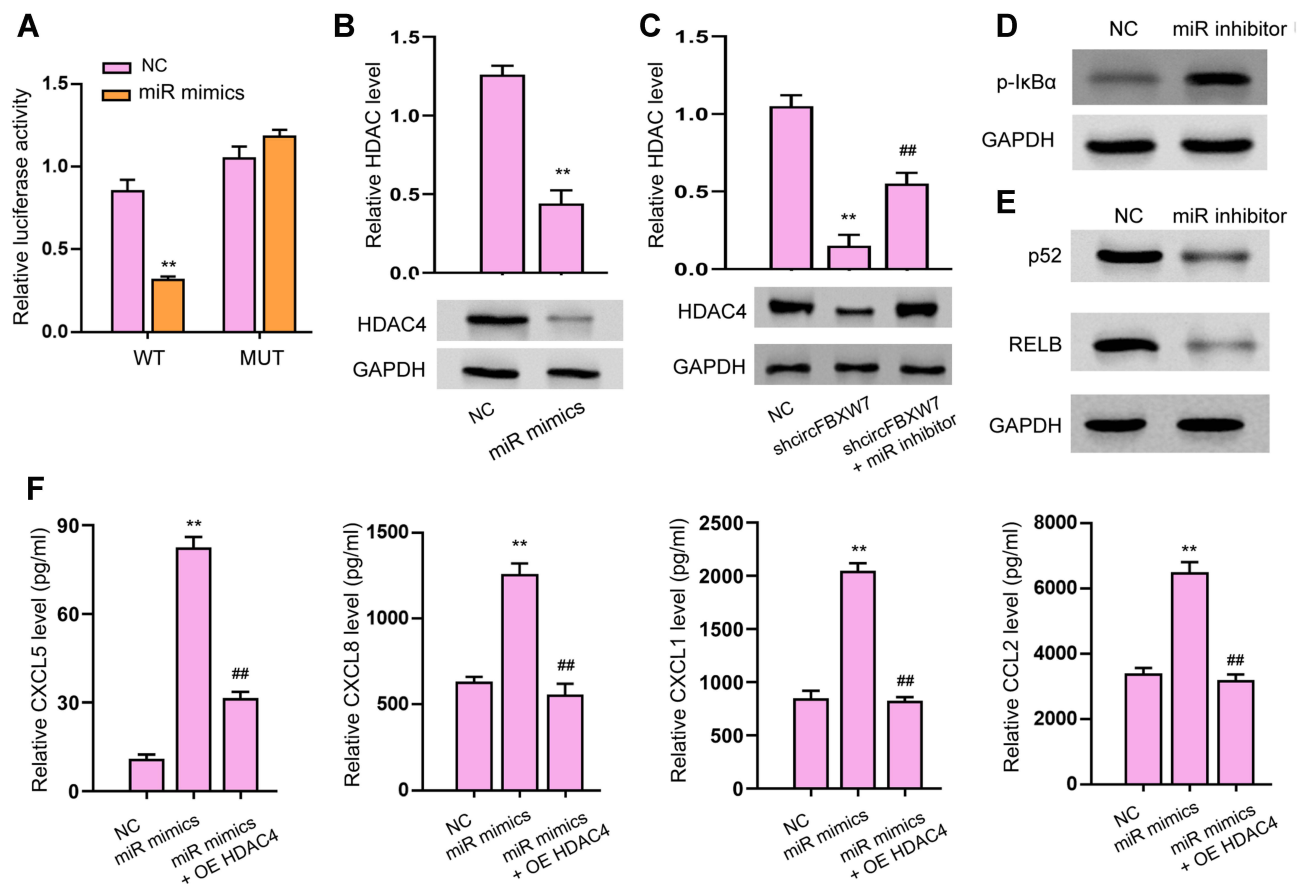


Figure 7 miR-216a-3p targets HDAC4 3'UTR to modulate inflammatory response in RA. (A–C) The luciferase activity of wild-type and mutated 3'UTR of HDAC4 was analyzed by dual-luciferase reporter assay. The protein level of HDAC4 was checked by Western blotting. (D and E) The phosphorylation of I κ B- α and the expression of p52 and RELB (E) were detected by Western blot assay. (F) The levels of CXCL5, CXCL8, CXCL1, and CCL2 were analyzed by ELISA assays. OE HDAC4, transfection with HDAC4 overexpressing vectors; ** $P < 0.01$ vsNC, ### $P < 0.01$ vs shcircFBXW7 or miR-216a-3p mimics (miR mimics).

Discussion

RA-FLSs play a critical role in the pathogenesis of RA owing to their aggressive phenotype, including boosted proliferation and invasion, and apoptosis arrest. Moreover, RA-FLSs also promote the secretion of various inflammatory cytokines, chemokines, and proteases including CXCL1, TNF- α , IL-1 β , and MMPs, and disrupts the extracellular matrix composites, and consequently causes joint destruction.^{4,32} Studies have reported that cytokines such as the TNF- α , interleukin family including the IL-1, IL-6, IL-10, and IL-18 and so on, and the chemokine families including C, CC, CXC, and CX₃C family, are closely involved in inflammation of joints.^{33,34} Hence, targeting RA-FLSs and ameliorating inflammatory responses is a plausible way for RA therapy.

In this work, we observed a decreased expression of circFBXW7 in synovial tissues of RA patients, in comparison with that from healthy donors. Our data indicated that

the circFBXW7 could be delivered by exosomes from MSCs to RA-FLSs, suppressed cell proliferation, migration, and invasion, simultaneously downregulated inflammatory cytokines including TNF- α , IL-1, IL-6, and IL-8. Study on in vivo model further confirmed the therapeutic effects of exosomal circFBXW7 against RA, manifested by alleviated tissue damage, suppressed expression of β -catenin and c-Myc, as well as downregulated secretion of inflammatory factors. Previous studies have suggested the ability of MSCs-derived exosomes could deliver functional factors to treat various diseases. For example, MSC-derived exosomal glutathione peroxidase 1 reduced oxidative stress and apoptosis and performed hepatoprotective effects.³⁵ MSC exosomes also exhibit immunomodulatory and regenerative potency, hence were regarded as new perspectives for treatment of cartilage injuries and osteoarthritis.³⁶ Exosomal CD73 from MSCs activates AKT and ERK signaling and osteochondral regeneration.³⁷

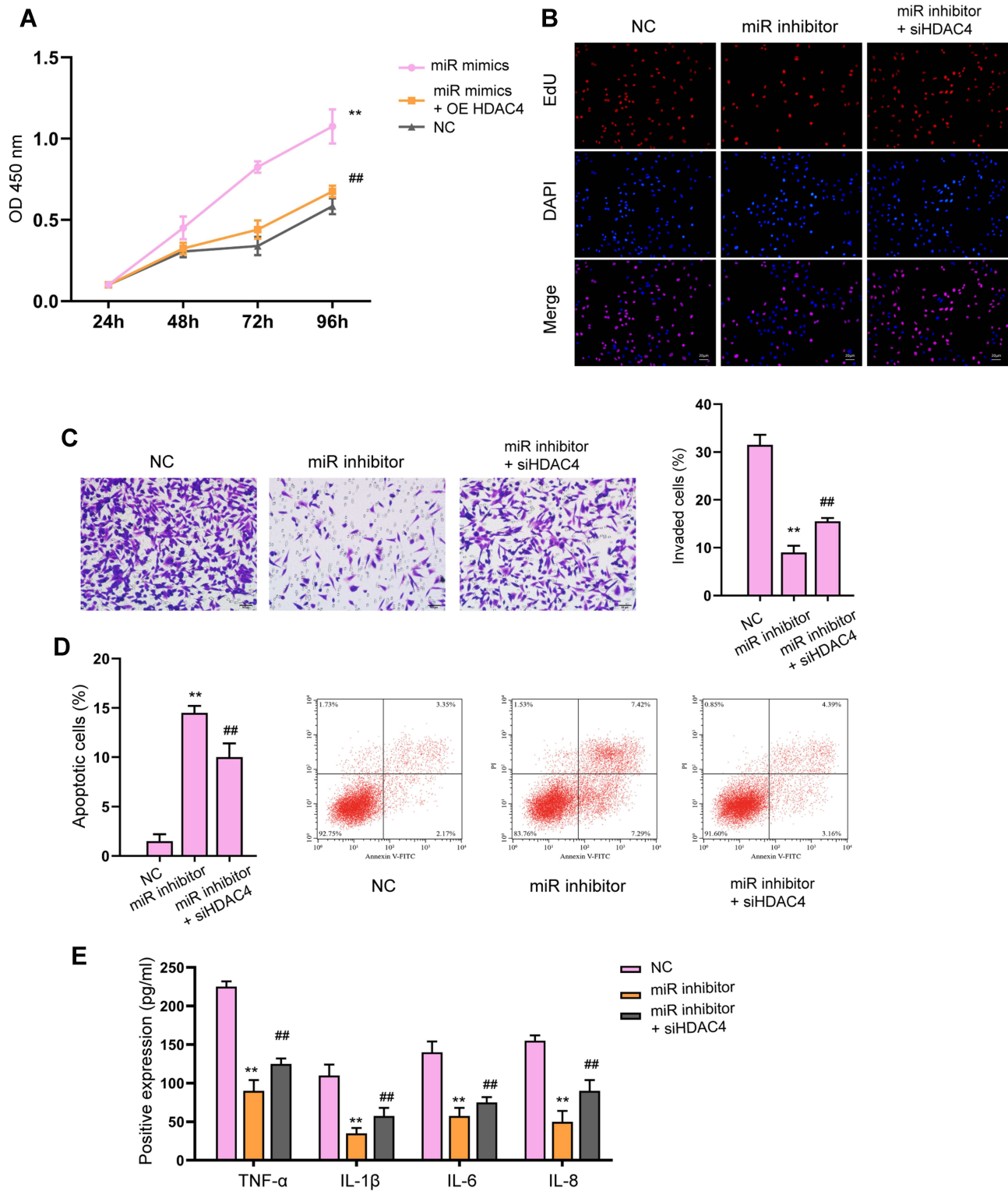


Figure 8 Knockdown of HDAC4 reverses the cellular function of miR-216a-3p inhibitor. **(A and B)** The cell viability and proliferation were measured by CCK-8 **(A)** and EdU assay, respectively. **(C)** The cell invasion was assessed by transwell. **(D)** Cell apoptosis determined by flow cytometry. **(E)** The levels of TNF- α , IL-1 β , IL-6 and IL-8 were analyzed by ELISA assay. ** $P < 0.01$ vs NC, ## $P < 0.01$ vs miR-216a-3p inhibitor.

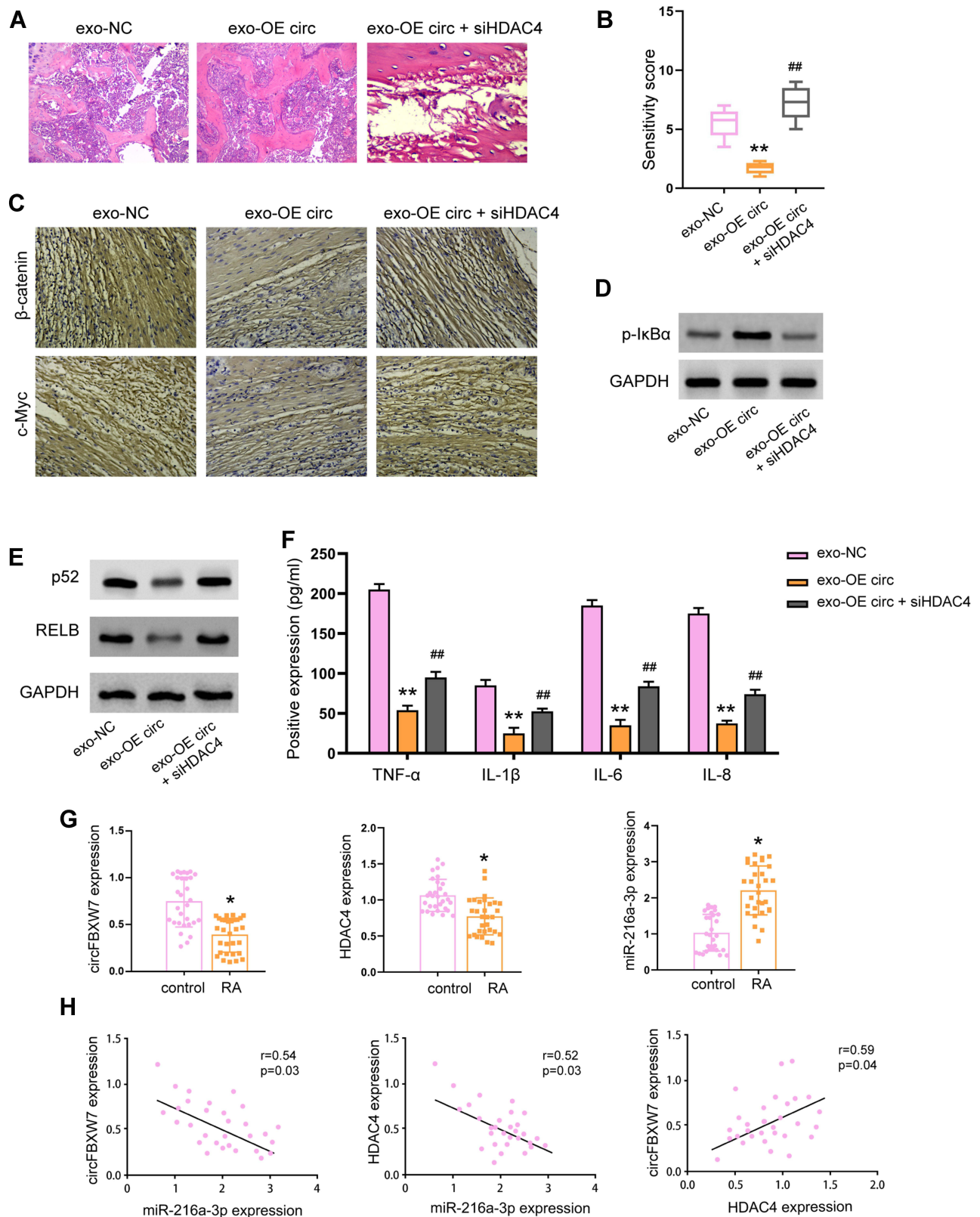


Figure 9 Knockdown of HDAC4 abolished the protective function of exosomal-circFBXW7 in RA model. The RA rat model was constructed and treated with exosomal circFBXW7 (exo-OE circ) or negative control (exo-NC), along with or without siHDAC4. **(A and B)** The pathological changes were analyzed by H&E staining. **(C)** The levels of β-catenin and c-Myc in synovium were measured by immunohistochemical staining. **(D and E)** The phosphorylation of IκB-α and the expression of p52 and RELB **(E)** were detected by Western blot assay. **(F)** The levels of TNF-α, IL-1β, IL-6, and IL-8 were checked by ELISA assay. ** $P < 0.01$. **(G)** Levels of circFBXW7, miR-216a-3p and HDAC4 in patients with RA was determined by qRT-PCR. **(H)** Correlation between circFBXW7, miR-216a-3p and HDAC4 was determined by Pearson analysis. * $P < 0.05$, ** $P < 0.01$ vs exo-NC, ### $P < 0.01$ vs exo-OE circ.

We next investigated the possible downstream mechanisms involved in the function of exosomal circFBXW7 in RA. It is known that circRNAs commonly function through sponging miRNAs. Previous studies also suggested that circFBXW7 sponges miR-197-3p and encodes a FBXW7-185aa protein, as well as inhibit c-Myc level to suppress breast cancer development.¹⁹ Similarly, upregulation of circFBXW7 reduced the stability of c-Myc, and positively associated with overall survival of glioma patients.²⁰ We found that circFBXW7 directly interacted with miR-216a-3p. Administration of miR-216a-3p abolished the therapeutic effects of exosomal circFBXW7 in RA-FLSs. Meanwhile, this study did not mention the changes of circRNA expression profile of RAFLS after circFBXW7 intervention, and the specific molecular functions of these circRNAs, which still need to be further studied. The effect of biologic agents on circFBXW7 should be explored in the future. CircFBXW7 encoded FBXW7-185aa protein and the expression and correlation of FBXW7-185aa protein with RA need to be identified. We failed to observe the effect of exosomal-FBXW7 on the proliferation and migration of fibroblast-like synoviocytes in vitro. The effect of exosomal-FBXW7 on RNA should be validated in vivo in the future investigations. MiR-216a-3p was reported to target the RUNX1 and activate NF- κ B signaling to regulate gastric cancer cell proliferation and invasion. Song H and colleagues reported that miR-216a-3p facilitated MSCs to differentiate into type II alveolar epithelial cells, which consequently elevated expression of pro-inflammatory factors including IL-1, TNF- α , and INF- α , and reduced anti-inflammatory factor such as IL-10.³⁸ These reports further supported our findings that miR-216a-3p promotes inflammation during RA. We also spotted elevated expression of HDAC4, the histone deacetylase that epigenetically regulates gene expression. Knockdown of HDAC4 abolished the therapeutic functions of exosomal circFBXW7 and miR-216a-3p inhibitor against the progressive phenotype of RA-FLSs. The previously reported inhibitory role of HDAC4 in RA progression supported our findings.

Conclusion

To summarize, our work determined the therapeutic role of circFBXW7 during RA development, explored the molecular mechanism of circFBXW7/miR-216a-3p/HDAC4 axis in suppressing the proliferation, migration, and inflammatory response of RA-FLSs. Our work provided a promising therapeutic target for RA.

Disclosure

The authors report no conflicts of interest in this work.

References

1. Josef SS, Daniel A, Iain BM. Rheumatoid arthritis. *Nat Rev Dis Primers*. 2018;4:18002.
2. McInnes IB, Schett G. Pathogenetic insights from the treatment of rheumatoid arthritis. *Lancet*. 2017;389(10086):2328–2337. doi:10.1016/S0140-6736(17)31472-1
3. Orr C, Vieira-Sousa E, Boyle DL, et al. Synovial tissue research: a state-of-the-art review. *Nat Rev Rheumatol*. 2017;13(10):630. doi:10.1038/nrrheum.2017.161
4. Bartok B, Firestein GS. Fibroblast-like synoviocytes: key effector cells in rheumatoid arthritis. *Immunol Rev*. 2010;233(1):233–255. doi:10.1111/j.0105-2896.2009.00859.x
5. Li N, Hua J. Interactions between mesenchymal stem cells and the immune system. *Cell Mol Life Sci*. 2017;74(13):2345–2360. doi:10.1007/s00018-017-2473-5
6. Di Nicola M, Carlo-Stella C, Magni M, et al. Human bone marrow stromal cells suppress T-lymphocyte proliferation induced by cellular or nonspecific mitogenic stimuli. *Blood*. 2002;99(10):3838–3843. doi:10.1182/blood.V99.10.3838
7. Corcione A, Benvenuto F, Ferretti E, et al. Human mesenchymal stem cells modulate B-cell functions. *Blood*. 2006;107(1):367–372. doi:10.1182/blood-2005-07-2657
8. Spaggiari GM, Capobianco A, Abdelrazik H, Becchetti F, Mingari MC, Moretta L. Mesenchymal stem cells inhibit natural killer-cell proliferation, cytotoxicity, and cytokine production: role of indoleamine 2,3-dioxygenase and prostaglandin E2. *Blood*. 2008;111(3):1327–1333. doi:10.1182/blood-2007-02-074997
9. Spaggiari GM, Abdelrazik H, Becchetti F, Moretta L. MSCs inhibit monocyte-derived DC maturation and function by selectively interfering with the generation of immature DCs: central role of MSC-derived prostaglandin E2. *Blood*. 2009;113(26):6576–6583. doi:10.1182/blood-2009-02-203943
10. Lopez-Santalla M, Fernandez-Perez R, Garin MI. Mesenchymal stem/stromal cells for rheumatoid arthritis treatment: an update on clinical applications. *Cells*. 2020;9(8):1852. doi:10.3390/cells9081852
11. Luque-Campos N, Contreras-Lopez RA, Jose Paredes-Martinez M, et al. Mesenchymal stem cells improve rheumatoid arthritis progression by controlling memory T cell response. *Front Immunol*. 2019;10:798. doi:10.3389/fimmu.2019.00798
12. Mead B, Tomarev S. Bone marrow-derived mesenchymal stem cells-derived exosomes promote survival of retinal ganglion cells through miRNA-dependent mechanisms. *Stem Cells Transl Med*. 2017;6(4):1273–1285. doi:10.1002/sctm.16-0428
13. Zhang L, Yu D. Exosomes in cancer development, metastasis, and immunity. *Biochim Biophys Acta Rev Cancer*. 2019;1871(2):455–468. doi:10.1016/j.bbcan.2019.04.004
14. Wortzel I, Dror S, Kenific CM, Lyden D. Exosome-mediated metastasis: communication from a distance. *Dev Cell*. 2019;49(3):347–360. doi:10.1016/j.devcel.2019.04.011
15. Kalluri R. The biology and function of exosomes in cancer. *J Clin Invest*. 2016;126(4):1208–1215. doi:10.1172/JCI81135
16. Salzman J, Gawad C, Wang PL, Lacayo N, Brown PO. Circular RNAs are the predominant transcript isoform from hundreds of human genes in diverse cell types. *PLoS One*. 2012;7(2):e30733. doi:10.1371/journal.pone.0030733
17. Huang XY, Huang ZL, Huang J, et al. Exosomal circRNA-100338 promotes hepatocellular carcinoma metastasis via enhancing invasiveness and angiogenesis. *J Exp Clin Cancer Res*. 2020;39(1):20. doi:10.1186/s13046-020-1529-9

18. Wang Y, Liu J, Ma J, et al. Exosomal circRNAs: biogenesis, effect and application in human diseases. *Mol Cancer*. 2019;18(1):116. doi:10.1186/s12943-019-1041-z
19. Ye F, Gao G, Zou Y, et al. circFBXW7 inhibits malignant progression by sponging miR-197-3p and encoding a 185-aa protein in triple-negative breast cancer. *Mol Ther Nucleic Acids*. 2019;18:88–98. doi:10.1016/j.omtn.2019.07.023
20. Yang Y, Gao X, Zhang M, et al. Novel role of FBXW7 circular RNA in repressing glioma tumorigenesis. *J Natl Cancer Inst*. 2018;110(3):304–315. doi:10.1093/jnci/djx166
21. Dong Y, Qiu T, Xuan Y, et al. circFBXW7 attenuates malignant progression in lung adenocarcinoma by sponging miR-942-5p. *Transl Lung Cancer Res*. 2021;10(3):1457–1473. doi:10.21037/tlcr-21-230
22. Xu Y, Qiu A, Peng F, Tan X, Wang J, Gong X. Exosomal transfer of circular RNA FBXW7 ameliorates the chemoresistance to oxaliplatin in colorectal cancer by sponging miR-18b-5p. *Neoplasma*. 2021;68(1):108–118. doi:10.4149/neo_2020_200417N414
23. Bi X, Guo XH, Mo BY, et al. LncRNA PICSAR promotes cell proliferation, migration and invasion of fibroblast-like synoviocytes by sponging miRNA-4701-5p in rheumatoid arthritis. *EBioMedicine*. 2019;50:408–420. doi:10.1016/j.ebiom.2019.11.024
24. Chen J, Liu M, Luo X, et al. Exosomal miRNA-486-5p derived from rheumatoid arthritis fibroblast-like synoviocytes induces osteoblast differentiation through the Tob1/BMP/Smad pathway. *Biomater Sci*. 2020;8(12):3430–3442. doi:10.1039/C9BM01761E
25. Tavasolian F, Hosseini AZ, Soudi S, Naderi M. miRNA-146a Improves immunomodulatory effects of MSC-derived exosomes in rheumatoid arthritis. *Curr Gene Ther*. 2020;20(4):297–312. doi:10.2174/1566523220666200916120708
26. Vega RB, Matsuda K, Oh J, et al. Histone deacetylase 4 controls chondrocyte hypertrophy during skeletogenesis. *Cell*. 2004;119(4):555–566. doi:10.1016/j.cell.2004.10.024
27. Zhang X, Qi Z, Yin H, Yang G. Interaction between p53 and Ras signaling controls cisplatin resistance via HDAC4- and HIF-1 α -mediated regulation of apoptosis and autophagy. *Theranostics*. 2019;9(4):1096–1114. doi:10.7150/thno.29673
28. Kong Q, Hao Y, Li X, Wang X, Ji B, Wu Y. HDAC4 in ischemic stroke: mechanisms and therapeutic potential. *Clin Epigenetics*. 2018;10(1):117. doi:10.1186/s13148-018-0549-1
29. Mielcarek M, Zielonka D, Carnemolla A, Marcinkowski JT, Guidez F. HDAC4 as a potential therapeutic target in neurodegenerative diseases: a summary of recent achievements. *Front Cell Neurosci*. 2015;9:42. doi:10.3389/fncel.2015.00042
30. Shao L, Hou C. miR-138 activates NF- κ B signaling and PGRN to promote rheumatoid arthritis via regulating HDAC4. *Biochem Biophys Res Commun*. 2019;519(1):166–171. doi:10.1016/j.bbrc.2019.08.092
31. Wu X, Showiheen SAA, Sun AR, et al. Exosomes extraction and identification. *Methods Mol Biol*. 2019;2054:81–91.
32. Nygaard G, Firestein GS. Restoring synovial homeostasis in rheumatoid arthritis by targeting fibroblast-like synoviocytes. *Nat Rev Rheumatol*. 2020;16(6):316–333. doi:10.1038/s41584-020-0413-5
33. McInnes IB, Buckley CD, Isaacs JD. Cytokines in rheumatoid arthritis - shaping the immunological landscape. *Nat Rev Rheumatol*. 2016;12(1):63–68. doi:10.1038/nrrheum.2015.171
34. Koch AE. Chemokines and their receptors in rheumatoid arthritis: future targets? *Arthritis Rheum*. 2005;52(3):710–721. doi:10.1002/art.20932
35. Yan Y, Jiang W, Tan Y, et al. hucMSC Exosome-Derived GPX1 Is Required for the Recovery of Hepatic Oxidant Injury. *Mol Ther*. 2017;25(2):465–479. doi:10.1016/j.ymthe.2016.11.019
36. Toh WS, Lai RC, Hui JHP, Lim SK. MSC exosome as a cell-free MSC therapy for cartilage regeneration: implications for osteoarthritis treatment. *Semin Cell Dev Biol*. 2017;67:56–64. doi:10.1016/j.semdb.2016.11.008
37. Zhang S, Chuah SJ, Lai RC, Hui JHP, Lim SK, Toh WS. MSC exosomes mediate cartilage repair by enhancing proliferation, attenuating apoptosis and modulating immune reactivity. *Biomaterials*. 2018;156:16–27. doi:10.1016/j.biomaterials.2017.11.028
38. Song H, Lu HN, Chen X, Jiang XF, Yang Y, Feng J. MiR-216a-3p promotes differentiation of BMMSCs into ACE II cells via Wnt/ β -catenin pathway. *Eur Rev Med Pharmacol Sci*. 2018;22(22):7849–7857. doi:10.26355/eurrev_201811_16410

Journal of Inflammation Research

Publish your work in this journal

The Journal of Inflammation Research is an international, peer-reviewed open-access journal that welcomes laboratory and clinical findings on the molecular basis, cell biology and pharmacology of inflammation including original research, reviews, symposium reports, hypothesis formation and commentaries on: acute/chronic inflammation; mediators of inflammation; cellular processes; molecular

mechanisms; pharmacology and novel anti-inflammatory drugs; clinical conditions involving inflammation. The manuscript management system is completely online and includes a very quick and fair peer-review system. Visit <http://www.dovepress.com/testimonials.php> to read real quotes from published authors.

Submit your manuscript here: <https://www.dovepress.com/journal-of-inflammation-research-journal>

Dovepress